Self-Cleaning Materials

DOI: 10.1002/anie.201204608

Self-Cleaning Functional Molecular Materials**

M. B. Avinash, Elisabeth Verheggen, Carsten Schmuck, and T. Govindaraju**

The controlled self-assembly of small molecules into well-defined, ordered nano- and microstructures is of current interest for potential applications in photavoltaics,[1] photonic crystals,[2] tissue engineering,[3] single-cell analysis,[4] microreactors,[5] and superhydrophobic coatings.[6] This bottom-up molecular assembly approach has been elegantly utilized by nature to form a variety of functional nanomaterials.[7] However, it is only now that chemists have begun to understand the underlying supramolecular design principles[8] in an ongoing effort to construct ordered two-dimensional (2D) or three-dimensional (3D) patterns and arrays, which could ultimately lead to complex architectures and functions. In this context, superhydrophobic surfaces in particular have come into focus in recent years, partly by the motivation to mimic nature and owing to their promising applications.[9] Over the years, a variety of chemical and physical methods for the fabrication of rough surfaces with subsequent low-surface-energy coatings have been explored by lithography,[10] sublimation,[11] plasma techniques,[12] self-assembled monolayers (SAM),[13] and electrochemical methods.[14] Furthermore, the so called breath-figure technique (BFT)[15] has also been explored owing to its simple solution processability, robustness, and the excellent tunability of size over three orders of magnitude (nm to μm). When a solution is drop-cast on a surface under humid air, the evaporation of the volatile solvent facilitates condensation of water droplets on the cold surface. This evaporative cooling and subsequent solidification of the solute under favorable conditions produces highly ordered arrays of well-defined cavities with diameters of 50 nm to 20 μm, called breath-figure arrays. However, the use of BFT has been limited to date to certain classes of macromolecules, such as star polymers,[16] cross-linked star polymers,[17] hyperbranched polymers,[18] conjugated polymers,[19] and dendronized polymers,[20] with an exception of only a few organogelators.[21] It has been argued that viscous polymer solutions with additional polar functionalities are required in BFT to form a stable interface with the water droplet.[21a] In contrast, small molecules either crystallize or unspecifically aggregate and thus lack the ability to stabilize water rafts.[22] Herein, we report our serendipitous discovery that a naphthalene diimide (NDI)-based molecule **1** forms highly-ordered self-assembled breath-figure arrays from dichloromethane solvent. Depending on the concentration of **1**, the surface roughness of the self-assembled materials changes and thus the surface wettability for water can be varied from a contact angle of 60° to 135°. Furthermore, upon sputtering a thin layer of gold onto these microarrays, we could ultimately successfully mimic the self-cleaning properties of the lotus leaf (contact angle of 156° and tilt angle of 3°). Furthermore, fluorescent dyes, such as perylenediimide, rhodamine B, and coumarines, can be incorporated within the self-assembled microarrays of **1**, giving rise to highly fluorescent hydrophobic molecular materials.

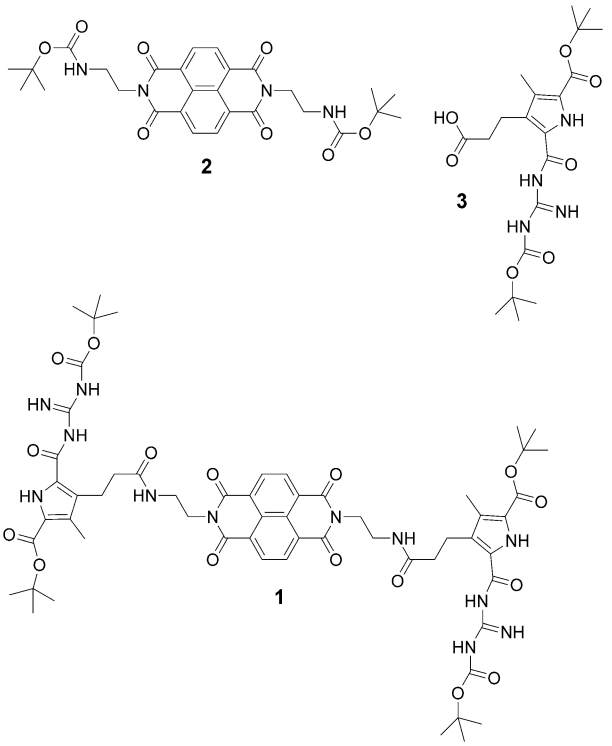

Compound **1** consists of a central naphthalene diimide core (NDI) functionalized with two N-*t*Boc (*tert*-butoxycarbonyl)-protected guanidinocarbonyl pyrrole (GCP) moieties. NDI is one of the most promising n-type organic semi-

[*] M. B. Avinash, Dr. T. Govindaraju
Bioorganic Chemistry Laboratory, New Chemistry Unit
Jawaharlal Nehru Centre for Advanced Scientific Research
Jakkur P.O., Bangalore 560064 (India)
Fax: (+91) 80-2208-2627
E-mail: tgraju@jncasr.ac.in
Homepage: http://www.jncasr.ac.in/tgraju/
E. Verheggen, Prof. Dr. C. Schmuck
Lehrstuhl für Organische Chemie 2, Fakultät für Chemie
Universität Duisburg-Essen
Universitätstrasse 7, 45141 Essen (Germany)
E-mail: carsten.schmuck@uni-due.de

[**] The authors thank Prof. C. N. R. Rao for constant support, JNCASR, IYBA-DBT Grant, and DST, India for financial support; Prof. G. U. Kulkarni for FESEM, Prof. S. K. Biswas, IISc for the contact-angle analyzer facility; and Selvi, Basavaraja, Suma, Chidanand, Vatsala, and Piyush for their help in various measurements.

Supporting information for this article is available on the WWW under http://dx.doi.org/10.1002/anie.201204608.

conductors with interesting optical and electronic properties[23] that have been exploited already in a variety of different applications.[24] The GCP group developed by one of us has found widespread use in self-assembling systems, even though most often in its deprotected dimerizing zwitterionic form.[25] A detailed description of the synthesis and characterization of **1** is given in the Supporting Information. Briefly, *t*Boc-deprotected **2** was coupled with **3** using a standard coupling reagent HBTU (O-benzotriazole-*N*,*N*,*N*′,*N*′-tetramethyluronium hexafluorophosphate) to obtain **1** in good yield.

The presence of both polar and non-polar functional groups in **1** ensures solubility in various organic solvents of different polarity index and should also allow for self-assembly. Indeed, **1** formed self-assembled structures of different morphologies from various organic solvents, as observed with field-emission scanning electron microscopy (FESEM) after drop-casting solutions of **1** onto silicon (111) substrates; particulate as well as film like morphologies are obtained from acetonitrile, random nanometer- and micrometer-sized particulate-like aggregates from tetrahydrofuran and dimethylsulfoxide, and discrete microwells from chloroform and carbon tetrachloride solutions (Supporting Information, Figure S1). To our surprise, from another chlorinated solvent, dichloromethane, **1** self-assembled into honeycomb-like microarrays (Figure 1 a). Interestingly, the sidewalls of these honeycomb-like microarrays were comprised of stack of nanobelts (Figure 1 b). Obviously, chlorinated solvents had a peculiar impact on the formation of microwells or microarrays. Previously we had encountered a similar situation wherein chlorinated co-solvents were found to be crucial in the formation of attoliter containers of NDIs.[26] In this earlier work, we had shown with the help of single-crystal X-ray data that chlorinated solvents interact with the carbonyl functionalities of NDI by means of halogen bonding interactions. Therefore, it is reasonable to assume that similar halogen bonding interactions occur with **1**, which might explain why **1** forms microwells and microarrays exclusively from chlorinated solvents. Furthermore, the exact morphology of the self-assembled structures depends on the concentration of **1** (Supporting Information, Figure S1). A 1 μM dichloromethane solution of **1** resulted only in discrete faint microwell-like features amongst groups of smaller microwells. With a 10-fold increase in concentration (10 μM), a microarray-like morphology formed from entangled nanobelts was observed. Increasing the concentration further to 100 μM led to a microarray with an internal diameter of less than 5 μm. Thus, as the concentration of **1** increases, the microarray structuring also increases with a gradual enhancement in the topographical thickness.

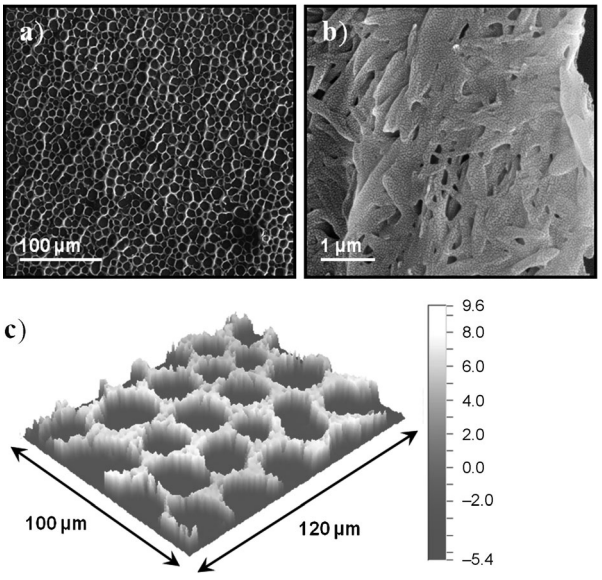

Figure 1. a) FESEM micrograph of **1** obtained by drop-casting a 1 mM dichloromethane solution. b) Higher-magnification FESEM micrograph showing a side wall within the honeycomb-like microarray. The side wall consists of nanobelt-like stacks; the particulate-like surface features are due to sputtered gold. c) An optical profiler 3D image depicting the dimensions of honeycomb-like microarrays obtained from 1 mM dichloromethane solution of **1**.

An optical profiler was utilized to obtain a 3D image of the microarrays obtained from a 1 mM solution. The section analysis revealed microarrays with an internal diameter of 10–25 μm with a topographical thickness of 10–15 μm (Figure 1 c). Moreover, to study the effect of the surface on morphogenesis, we also employed mica and glass as other substrates. On mica, microarrays were formed as well with an internal diameter ranging from 15 to 35 μm (Supporting Information, Figure S2). Furthermore, within these large microwells, smaller discrete microwells were observed that are most likely due to smaller breath figures. On the contrary, a glass surface produced significantly smaller microwells of only 1 to 6 μm internal diameter, with the rest of the surface being covered with a network of belt like aggregates (Supporting Information, Figure S2).

To investigate the role of different molecular functionalities in **1** on morphogenesis, we also studied the self-assembly of the building blocks **2** and **3** and the *t*Boc-deprotected version of **2**, the direct precursor for **1** (Supporting Information, Figure S3). The *t*Boc-deprotected version of **2** was sparingly soluble in dichloromethane, and the resulting morphology obtained after drop-casting on a silicon substrate was random particulate in nature. Interestingly, a 1 mM dichloromethane solution of **3** resulted in a faint honeycomb-like structure of 10–50 μm internal diameter. However, this microarray lacked topographical thickness as observed with **1**. Unlike **3**, a dichloromethane solution of **2** (1 mM) produced microwells of 3 to 30 μm internal diameter. Chloroform solutions of **2** (1 mM) were found to produce microwells of 4 to 10 μm internal diameter. These results clearly demonstrate that for the formation of well-ordered microarrays both chemical motifs in **1**, the NDI core and the GCP group, are required. The honeycomb-like features of **1** is thus most likely to emerge from the GCP groups, which allow extensive intermolecular hydrogen bonding allowing the formation of large self-assembled structures, whereas the NDI core in **1** seems to be the major contributor to the topographical thickness of the microarrays (probably by inducing π–π-stacking of these self-assembled structures).

A literature survey suggested a probable role of BFT for the formation of such honeycomb-like microarrays, even

though breath-figure arrays to date were mainly observed for polymers but not small low-molecular-weight compounds such as **1**. Nevertheless, to test the hypothesis whether BFT might be important for structure formation in our case, we studied the self-assembly of **1** in atmospheres with different relative humidity (RH). When a 1 mM dichloromethane solution of **1** was drop-cast on a silicon substrate in an inert atmosphere with about 0% RH, only random aggregates without any indication for the formation of microarrays were observed (Supporting Information, Figure S4). This strongly indicates the importance of humidity as required in BFT. To study the effect of RH on microarray formation quantitatively, a set up was developed to maintain and control the humidity during the self-assembly process (for details, see the Supporting Information). Dichloromethane solutions of **1** were drop-cast under five different RH values of 35%, 50%, 65%, 80%, and 95%. At 35% RH, the wells of the microarrays had dimensions in the range of 40 to 100 μm (Supporting Information). However, the microwells were of uneven topographical thickness and most often the wells were fused with their neighbors. With increasing RH, significantly better structured microarrays were observed. Moreover, the internal diameter of the microwells decreased with increasing RH. To further elucidate the mechanism of microarray formation, dynamic light-scattering (DLS) measurements were performed. In a 1 mM dichloromethane solution of **1** self-assembled aggregates having a hydrodynamic diameter of about 220 nm are observed (Supporting Information, Figure S9). Upon increasing the concentration to 5 mM, even large aggregates of about 784 nm size among the smaller aggregates of about 161 nm were observed. Thus, **1** self-assembles into supramolecular polymeric aggregates in dichloromethane, which is most likely due to the strong hydrogen bonding of the GCP groups in this solvent. Furthermore, in more concentrated solutions the size of the aggregates increases significantly, which is probably due to the weaker π–π interactions of the NDI core. These findings now allow presenting a plausible mechanism for structure formation (Figure 2). Thus, when a dichloromethane solution of **1** is drop-cast on a substrate, the evaporative cooling owing to the evaporation of the volatile solvent dichloromethane causes a decrease in the surface temperature, which induces condensation of water vapors present in humid air. However, the condensed water droplets on the surface are stabilized and protected from coalescing by interaction with the self-assembled aggregates of **1** already present in solution. Upon further evaporation of dichloromethane, the hexagonally packed array of water rafts then induces the formation of self-assembled honeycomb-like microarrays of **1**. As the microscopy image of the walls of the microarrays shows (Figure 1b), the original aggregates in solution most likely consist of nanobelt-like structures. A representation of this breath-figure mechanism is shown in Figure 2. The presence of the different polar and aromatic functionalities in **1** is believed to synergistically stabilize both the self-assembled structures of **1** and the water droplets at their interface. The rigidity of the nanobelt-like aggregates of **1** then facilitates a hexagonal assembly around the water droplets, which is then responsible for the formation of distorted hexagonal cavities in the BFT microarrays. Furthermore, the breath-figure arrays produced from chlorinated solvents most likely involve halogen bonding. For such halogen bonding, carbonyl functionalities in **1** seem to play a crucial role.[15,26] Also the fact that dichloromethane is immiscible in water is important for BFT.

The enhanced surface roughness properties associated with nano- and microstructured surfaces is utilized by nature to control water wettability in different systems, such as lotus leaves, desert beetles, mosquito eyes, and water striders. As with increasing concentration of **1**, the topographical thickness and thus the surface roughness of the self-assembled microarrays increases, the wettability of the surfaces should decrease, accordingly turning the material into a hydrophobic coating. Indeed, the contact angle of a 4 μL water droplet increases gradually from 60° for the surface obtained from a 1 μM solution of **1** to 134° for a 1 mM solution (Figure 3). Thus, simply by varying the concentration of **1**, the surface wettability of the same material could be tuned from hydrophilic to strongly hydrophobic owing to concentration-dependent changes in the morphology and thus the roughness of the surface (Supporting Information, Figure S1).

To increase the hydrophobicity even further, a low-surface-energy coating of the microarray was produced by sputtering gold onto the surface (Figure 4). The sputtered gold was about 100 nm thick with circa 100 nm sized particulates (Supporting Information, Figure S5). The nanostructured gold coating not only serves as a stable inert coating on the self-assembled microarray surface but also allows for further chemical modifications of the microarrays using self-assembled monolayers of thiols (SAMs).[27] These can be simply obtained by immersing the gold covered surface in 5 mM ethanol solution of different thiols for a duration of 24 h.[28] We have used three different thiols in our experiments, namely 11-mercaptoundecanoic acid (MSH), 1*H*, 1*H*, 2*H*, 2*H*-perfluorodecanethiol (FSH; Figure 4), and 1-dodecanethiol (DSH) to provide SAMs with different chemical functionalities (MSH: negatively charged, FSH: fluorinated, DSH: nonpolar), which affect the surface wettability differently. The gold coating on the surface of the microarray obtained from a 1 mM dichloromethane solution of **1** exhibits a contact angle of 125° (Figure 3e), which is similar to the

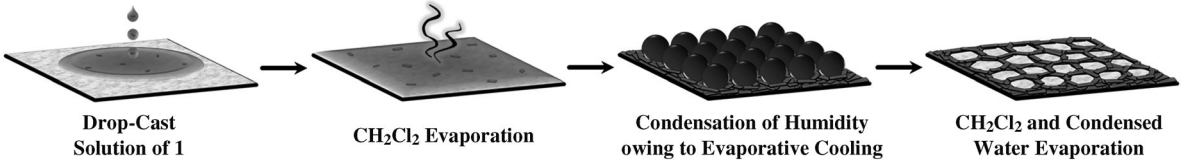

Figure 2. The formation of honeycomb-like microarrays from self-assembled structures of **1** by means of BFT. Not to scale.

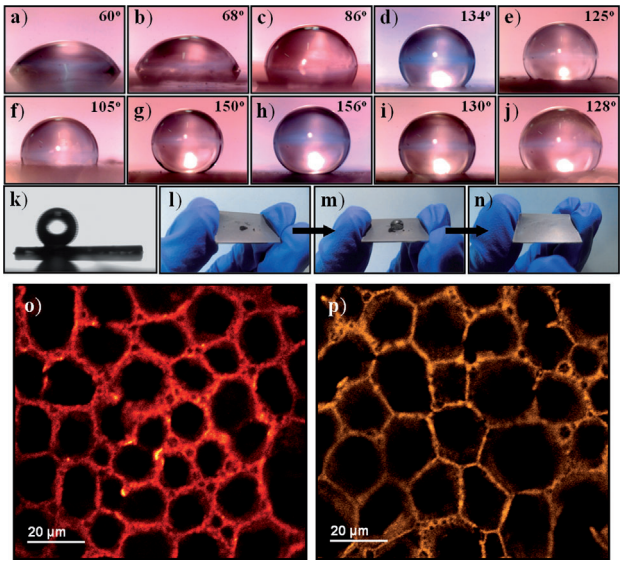

Figure 3. Optical images of the contact angle exhibited by a 4 μL water droplet on a microarray surface produced from: a) 1 μM CH_2Cl_2 solution; b) 10 μM CH_2Cl_2 solution; c) 100 μM CH_2Cl_2 solution; d) 1 mM CH_2Cl_2 solution; e) 1 mM CH_2Cl_2 solution followed by gold coating; f) 1 mM CH_2Cl_2 solution followed by gold coating and a SAM of 11-mercaptoundecanoic acid; g) 1 mM CH_2Cl_2 solution followed by gold coating and a SAM of 1-dodecanethiol; h) 1 mM CH_2Cl_2 solution followed by gold coating and a SAM of 1*H*,1*H*,2*H*,2*H*-perfluorodecanethiol; i) a mixture containing 10:1 ratio (1 mM:100 μM) of **1** and rhodamine B in CH_2Cl_2 ; and j) a mixture containing 10: 1 ratio (1 mM:100 μM) of **1** and isoleucinemethyl ester appended perylenediimide in CH_2Cl_2 . The values in (a) to (j) are the corresponding contact angles. k) Optical image showing the rolling of a water droplet for a tilt angle of 3°. l), m), and n) Images of a gold sputtered honeycomb-like microarray surface coated with 1*H*,1*H*,2*H*,2*H*-perfluorodecanethiol showing self-cleanability. Confocal micrographs obtained from o) a mixture containing 10:1 ratio (1 mM:100 μM) of **1** and rhodamine B in CH_2Cl_2 ; p) mixture containing 10:1 ratio (1 mM:100 μM) of **1** and isoleucine methyl ester appended perylenediimide in CH_2Cl_2.

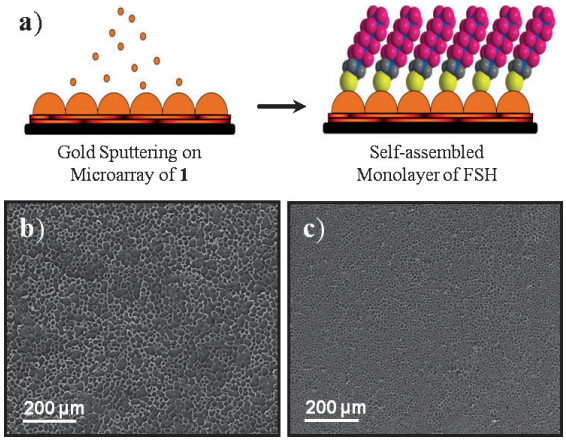

Figure 4. a) Gold sputtering and subsequent functionalization with SAM of FSH on microarray of **1**. FESEM micrographs of honeycomb-like microarrays produced at RH of b) 65% and c) 95%, after sputtered gold coating followed by a SAM of FSH.

noncovered surface (134°). The MSH coating gave a decreased contact angle of 105° owing to the presence of the terminal polar COOH groups (Figure 3 f). In contrast, the nonpolar DSH coating resulted in a superhydrophobic surface with an increased contact angle of 150° (Figure 3 g). The fluorinated FSH coating pushed the contact angle of the superhydrophobic surface even further to 156° (Figure 3 h). Artificial superhydrophobic surfaces are often not self-cleaning surfaces even though they have a large contact angle, because they suffer from a high tilt angle and high contact angle hysteresis. In contrast, the FSH coating on the microarray of **1** exhibits a tilt angle of only 3° and a very low contact angle hysteresis of only 1° (Figure 3 k). Accordingly, black carbon dust placed on the surface could be self-cleaned by water without any trace of remaining carbon dust or water stains (Figure 3 l–n).

Furthermore, to provide this material with additional interesting optical properties, we incorporated fluorescent dyes into the hierarchical molecular self-assemblies of **1**. Such dyes should be soluble in dichloromethane so that they can be mixed with **1** in specific proportions and still allow the formation of breath-figure arrays. As the self-assembled structure of **1** is partly based on π–π interactions, aromatic dyes seemed most attractive. As a first illustration, we thus incorporated rhodamine B (100 μM) in a dichloromethane solution of **1** (1 mM), which on drop-casting resulted again in a honeycomb-like microarray (Figure 3 o). The presence of the rhodamine dye did not interfere with structure formation but made the microarrays highly fluorescent. A cross-sectional analysis of the microarray at different topographical heights using fluorescent confocal microscopy confirmed a homogeneous distribution of the dye throughout the microarray (for more details, see the Supporting Information). Therefore, the dye is not only absorbed on the surface but an integral part of the self-assembled structure itself. The same finding was obtained with an isoleucine methyl ester appended perylenediimide (PDI) dye. The yellowish orange fluorescence of the PDI again appeared only along the walls of the microarray (Figure 3 p; for more details, see the Supporting Information). The contact angle for the microarrays with the incorporated rhodamine B and PDI were 130° (Figure 3 i) and 128° (Figure 3 j), respectively. These angles are more or less the same as of the non-functionalized microarrays (134°; Figure 3 d), confirming again that the dyes did not alter the self-assembly of **1** significantly. Furthermore, a blue fluorescent 7-amino-4-trifluoromethyl coumarin and a green fluorescent coumarin dye could also be incorporated into the microarrays similar to rhodamine B and the PDI. Unfortunately, fluorescent confocal micrographs for these coumarin dyes (absorption in the UV region) were hampered by reflections caused by the silicon substrate preventing a more detailed analysis of the distribution of the dyes within the microarrays.

In conclusion, the unexpected spontaneous hierarchical molecular assembly of a small low-molecular-weight naphthalenediimide derivative **1** into microarrays was achieved by a simple solution-processing technique (breath-figure technique). These arrays could be employed to fabricate self-cleaning surfaces with very low slide angle (3°) and contact angle hysteresis (1°). This finding is rather surprising as it was commonly believed that BFT cannot be used effectively for

small non-polymeric molecules. The molecular design could influence the formation of honeycomb-like microarrays and thereby provide better insights for future endeavors. However, it is known that in case of polymers, the internal diameter of the microarray formed using BFT increases linearly with increasing RH.[15] In contrast to these polymers, our results on **1** show that the cavity size actually decreases with increasing RH. Nevertheless, our work demonstrates that advanced functional molecular materials can be obtained, even from small molecules based on a simple and easy-to-use solution process. Furthermore, the resulting microstructures are very robust and can be easily functionalized by simply adding additional molecules into the solution as demonstrated by the incorporation of different dyes into the arrays. Using this approach and the three primary colors red, green, and blue, we are currently working towards white -light-emitting as well as other rainbow-colored hydrophobic decorative molecular materials alongside an effort to obtain nanoarrays for potential applications in electronics and miniaturized biochemical assays.

Received: June 13, 2012
Revised: August 2, 2012
Published online: September 11, 2012

Keywords: microarrays · molecular recognition · naphthalenediimides · self-assembled monolayers · self-cleaning materials

[1] E. S. Kwak, W. Lee, N.-G. Park, J. Kim, H. Lee, *Adv. Funct. Mater.* **2009**, *19*, 1093 – 1099.
[2] S. Kubo, Z.-Z. Gu, K. Takahashi, A. Fujishima, H. Segawa, O. Sato, *J. Am. Chem. Soc.* **2004**, *126*, 8314 – 8319.
[3] V. P. Shastri, I. Martin, R. Langer, *Proc. Natl. Acad. Sci. USA* **2000**, *97*, 1970 – 1975.
[4] M. A. Walling, J. R. E. Shepard, *Chem. Soc. Rev.* **2011**, *40*, 4049 – 4076.
[5] S. J. Haswell, V. Skelton, *TrAC Trends Anal. Chem.* **2000**, *19*, 389 – 395.
[6] X. Zhang, F. Shi, J. Niu, Y. Jiang, Z. Wang, *J. Mater. Chem.* **2008**, *18*, 621 – 633.
[7] a) C. Sanchez, H. Arribart, M. M. G. Guille, *Nat. Mater.* **2005**, *4*, 277 – 288; b) F. Xia, L. Jiang, *Adv. Mater.* **2008**, *20*, 2842 – 2858.
[8] a) T. Aida, E. W. Meijer, S. I. Stupp, *Science* **2012**, *335*, 813 – 817; b) S. Yagai, T. Seki, T. Karatsu, A. Kitamura, F. Würthner, *Angew. Chem.* **2008**, *120*, 3415 – 3419; *Angew. Chem. Int. Ed.* **2008**, *47*, 3367 – 3371; c) Y. Tidhar, H. Weissman, S. G. Wolf, A. Gulino, B. Rybtchinski, *Chem. Eur. J.* **2011**, *17*, 6068 – 6075; d) V. J. Bradford, B. L. Iverson, *J. Am. Chem. Soc.* **2008**, *130*, 1517 – 1524; e) H. Shao, J. Seifert, N. C. Romano, M. Gao, J. J. Helmus, C. P. Jaroniec, D. A. Modarelli, J. R. Parquette, *Angew. Chem.* **2010**, *122*, 7854 – 7857; *Angew. Chem. Int. Ed.* **2010**, *49*, 7688 – 7691; f) N. Sakai, R. Bhosale, D. Emery, J. Mareda, S. Matile, *J. Am. Chem. Soc.* **2010**, *132*, 6923 – 6925; g) M. B. Avinash, T. Govindaraju, *Adv. Mater.* **2012**, *24*, 3905 – 3922; h) T. Govindaraju, M. B. Avinash, *Nanoscale* **2012**, DOI: 10.1039/c2nr31167d.
[9] X. Yao, Y. Song, L. Jiang, *Adv. Mater.* **2011**, *23*, 719 – 734.
[10] D. Öner, T. J. McCarthy, *Langmuir* **2000**, *16*, 7777 – 7782.
[11] A. Nakajima, A. Fujishima, K. Hashimoto, T. Watanabe, *Adv. Mater.* **1999**, *11*, 1365 – 1368.
[12] S. R. Coulson, I. S. Woodward, J. P. S. Badyal, *Chem. Mater.* **2000**, *12*, 2031 – 2038.
[13] a) Y. Jiang, P. Wan, M. Smet, Z. Wang, X. Zhang, *Adv. Mater.* **2008**, *20*, 1972 – 1977; b) J. C. Love, B. D. Gates, D. B. Wolfe, K. E. Paul, G. M. Whitesides, *Nano Lett.* **2002**, *2*, 891 – 894.
[14] X. Zhang, F. Shi, X. Yu, H. Liu, Y. Fu, Z. Wang, L. Jiang, X. Li, *J. Am. Chem. Soc.* **2004**, *126*, 3064 – 3065.
[15] U. H. F. Bunz, *Adv. Mater.* **2006**, *18*, 973 – 989.
[16] H. T. Lord, J. F. Quinn, S. D. Angus, M. R. Whittaker, M. H. Stenzel, T. P. Davis, *J. Mater. Chem.* **2003**, *13*, 2819 – 2824.
[17] L. A. Connal, R. Vestberg, P. A. Gurr, C. J. Hawker, G. G. Qiao, *Langmuir* **2008**, *24*, 556 – 562.
[18] C. Liu, C. Gao, D. Yan, *Angew. Chem.* **2007**, *119*, 4206 – 4209; *Angew. Chem. Int. Ed.* **2007**, *46*, 4128 – 4131.
[19] B. Erdogan, L. Song, J. N. Wilson, J. O. Park, M. Srinivasarao, U. H. F. Bunz, *J. Am. Chem. Soc.* **2004**, *126*, 3678 – 3679.
[20] C. X. Cheng, Y. Tian, Y. Q. Shi, R. P. Tang, F. Xi, *Langmuir* **2005**, *21*, 6576 – 6581.
[21] a) J. H. Kim, M. Seo, S. Y. Kim, *Adv. Mater.* **2009**, *21*, 4130 – 4133; b) S. S. Babu, S. Mahesh, K. K. Kartha, A. Ajayaghosh, *Chem. Asian J.* **2009**, *4*, 824 – 829; c) Y. Yu, Y. Ma, *Soft Matter* **2011**, *7*, 884 – 886.
[22] a) M. Du, P. Zhu, X. Yan, Y. Su, W. Song, J. Li, *Chem. Eur. J.* **2011**, *17*, 4238 – 4245; b) Y.-F. Gao, Y.-J. Huang, S.-Y. Xu, W.-J. Ouyang, Y.-B. Jiang, *Langmuir* **2011**, *27*, 2958 – 2964; c) J. Chen, X. Yan, Q. Zhao, L. Li, F. Huang, *Polym. Chem.* **2012**, *3*, 458 – 462.
[23] a) S. V. Bhosale, C. H. Jani, S. J. Langford, *Chem. Soc. Rev.* **2008**, *37*, 331 – 342; b) R. Bhosale, J. Míšek, N. Sakai, S. Matile, *Chem. Soc. Rev.* **2010**, *39*, 138 – 149; c) J. H. Oh, S.-L. Suraru, W.-Y. Lee, M. Könemann, H. W. Höffken, C. Röger, R. Schmidt, Y. Chung, W.-C. Chen, F. Würthner, Z. Bao, *Adv. Funct. Mater.* **2010**, *20*, 2148 – 2156; d) B. A. Jones, A. Facchetti, M. R. Wasielewski, T. J. Marks, *J. Am. Chem. Soc.* **2007**, *129*, 15259 – 15278; e) H. E. Katz, J. Johnson, A. J. Lovinger, W. Li, *J. Am. Chem. Soc.* **2000**, *122*, 7787 – 7792; f) J. G. Laquindanum, H. E. Katz, A. Dodabalapur, A. J. Lovinger, *J. Am. Chem. Soc.* **1996**, *118*, 11331 – 11332.
[24] a) N. Sakai, J. Mareda, E. Vauthey, S. Matile, *Chem. Commun.* **2010**, *46*, 4225 – 4237; b) M. B. Avinash, T. Govindaraju, *Nanoscale* **2011**, *3*, 2536 – 2543; c) B. M. Aveline, S. Matsugo, R. W. Redmond, *J. Am. Chem. Soc.* **1997**, *119*, 11785 – 11795; d) V. Tumiatti, A. Milelle, A. Minarini, M. Micco, A. G. Campani, L. Roncuzzi, D. Baiocchi, J. Marinello, G. Capranico, M. Zini, C. Stefanelli, C. Melchiorre, *J. Med. Chem.* **2009**, *52*, 7873 – 7877.
[25] a) C. Schmuck, W. Wienand, *J. Am. Chem. Soc.* **2003**, *125*, 452 – 459; b) G. Gröger, V. Stepanenko, F. Würthner, C. Schmuck, *Chem. Commun.* **2009**, 698 – 700; c) G. Gröger, W. Meyer-Zaika, C. Böttcher, F. Gröhn, C. Ruthard, C. Schmuck, *J. Am. Chem. Soc.* **2011**, *133*, 8961 – 8971.
[26] M. B. Avinash, T. Govindaraju, *Adv. Funct. Mater.* **2011**, *21*, 3875 – 3882.
[27] C. Vericat, M. E. Vela, G. Benitez, P. Carro, R. C. Salvarezza, *Chem. Soc. Rev.* **2010**, *39*, 1805 – 1834.
[28] a) J. C. Love, L. A. Estroff, J. K. Kriebel, R. G. Nuzzo, G. M. Whitesides, *Chem. Rev.* **2005**, *105*, 1103 – 1169; b) T. Govindaraju, P. J. Bertrics, N. L. Abbott, R. T. Raines, *J. Am. Chem. Soc.* **2007**, *129*, 11223 – 11231.

